

A blocking monoclonal antibody to CCL24 alleviates liver fibrosis and inflammation in experimental models of liver damage

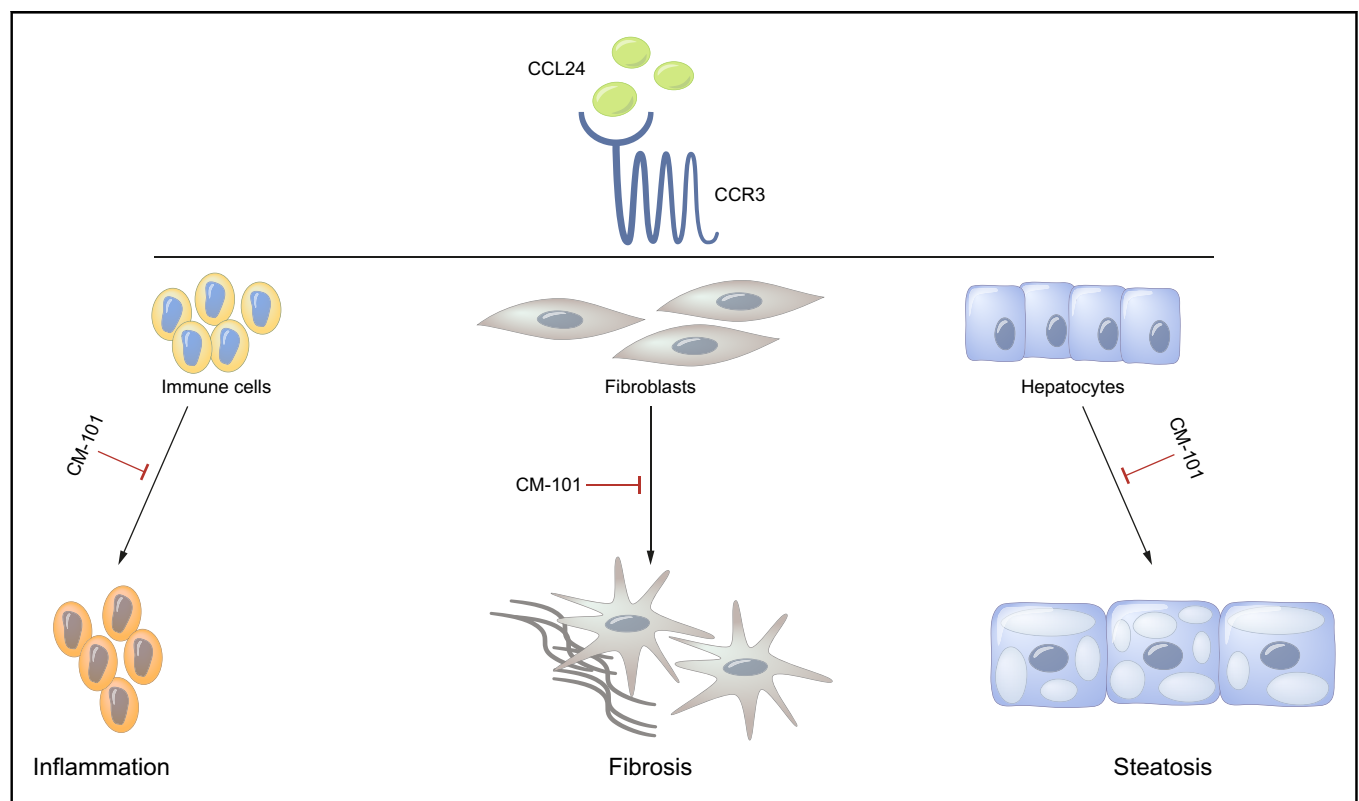
Authors

Michal Segal-Salto, Neta Barashi, Avi Katav, Vicktoria Edelshtein, Arnon Aharon, Sharon Hashmueli, Jacob George, Yaakov Maor, Massimo Pinzani, Dan Haberman, Andrew Hall, Scott Friedman, Adi Mor

Correspondence

adimor@chemomab.com (A. Mor).

Graphical abstract



Highlights

- CCL24 is a chemokine that regulates inflammatory and fibrotic activities through its receptor, CCR3.
- Significant expression of CCL24 and CCR3 were found in liver biopsies and blood samples from patients with NAFLD/NASH.
- CM-101, a monoclonal antibody that selectively targets CCL24, significantly attenuates fibrotic and inflammatory processes.
- Blocking CCL24 may have a potential therapeutic effect in NASH and liver fibrosis.

Lay summary

CCL24 is a chemokine that regulates inflammation and fibrosis. It was found to be significantly expressed in patients with non-alcoholic steatohepatitis, in whom it regulates profibrotic processes in the liver. Herein, we show that blockade of CCL24 using a monoclonal antibody robustly attenuated liver fibrosis and inflammation in animal models, thus suggesting a potential therapeutic role for an anti-CCL24 agent.



A blocking monoclonal antibody to CCL24 alleviates liver fibrosis and inflammation in experimental models of liver damage

Michal Segal-Salto,¹ Neta Barashi,¹ Avi Katav,¹ Vicktoria Edelshtein,¹ Arnon Aharon,¹ Sharon Hashmueli,¹ Jacob George,² Yaakov Maor,³ Massimo Pinzani,^{4,5} Dan Haberman,² Andrew Hall,^{4,5} Scott Friedman,⁶ Adi Mor^{1,*}

¹ChemomAb, Tel Aviv, Israel; ²Heart Center, Kaplan Medical Center, Rehovot, Affiliated to the Hebrew University, Jerusalem, Israel; ³Institute of Gastroenterology and Hepatology, Kaplan Medical Center, Rehovot, Israel; ⁴UCL Institute for Liver and Digestive Health, University College of London, London, UK; ⁵Sheila Sherlock Liver Centre, Royal Free London NHS Foundation Trust, London, UK; ⁶Division of Liver Diseases, Department of Medicine, Icahn School of Medicine at Mount Sinai, NY, USA

JHEP Reports 2020. <https://doi.org/10.1016/j.jhepr.2019.100064>

Background & Aims: C-C motif chemokine ligand 24 (CCL24) is a chemokine that regulates inflammatory and fibrotic activities through its receptor, C-C motif chemokine receptor (CCR3). The aim of the study was to evaluate the involvement of the CCL24-CCR3 axis in liver fibrosis and inflammation and to assess the potential of its blockade, by a monoclonal anti-CCL24 antibody, as a therapeutic strategy for non-alcoholic steatohepatitis (NASH) and liver fibrosis.

Methods: Expression of CCL24 and CCR3 was evaluated in liver biopsies and blood samples. CCL24 involvement in NAFLD/NASH pathogenesis was assessed in *Ccl24* knockout mouse using the methionine-choline deficient (MCD) diet experimental model. Antifibrotic and anti-inflammatory effects of CM-101 were tested in the MCD and STAM mouse models and in the thioacetamide (TAA) model in rats. Liver enzymes, liver morphology, histology and collagen deposition, as well as fibrosis- and inflammation-related protein expression were assessed. Activation of hepatic stellate cells (HSCs) was evaluated in the human LX2 cell line.

Results: Patients with NASH and advanced NAFLD exhibited significant expression of both CCL24 and CCR3 in liver and blood samples. In the experimental MCD-diet model, *Ccl24* knockout mice showed an attenuated liver damage response compared to wild-type mice, exhibiting reduced histological NAFLD activity scores and fibrosis, as well as lower levels of liver enzymes. Blocking CCL24 using CM-101 robustly reduced liver damage in 3 experimental animal models (MCD, STAM and TAA), as demonstrated by attenuation of liver fibrosis and NAFLD activity score. Furthermore, blocking CCL24 by CM-101 significantly inhibited CCL24-induced HSC motility, α -SMA expression and pro-collagen I secretion.

Conclusion: Our results reveal that blocking CCL24 significantly attenuates liver fibrosis and inflammation and may have a potential therapeutic effect in patients with NASH and/or liver fibrosis.

© 2019 The Author(s). Published by Elsevier B.V. on behalf of European Association for the Study of the Liver (EASL). This is an open access article under the CC BY-NC-ND license (<http://creativecommons.org/licenses/by-nc-nd/4.0/>).

Introduction

Non-alcoholic fatty liver disease (NAFLD) is the most common chronic liver disease affecting up to 30% of the adult population and 70–80% of individuals who are obese and diabetic.¹ It is a heterogeneous disease that may range from a relatively mild and subtle disease (hepatic steatosis) to a much more active and progressive disease, designated non-alcoholic steatohepatitis (NASH). Many individuals with simple steatosis do not progress to a more severe disease, however, NASH can progress to both cirrhosis and end-stage liver disease. Currently, there are no medications approved by the Food and Drug Administration or European Medicines Agency for the treatment of NAFLD or

NASH,^{2,3} and treatment guidelines focus on lifestyle interventions.¹

Liver fibrosis, a major marker of the progression from NAFLD to NASH and of disease severity, is the process of excessive accumulation of extracellular matrix proteins, predominantly collagen, which occurs as results of liver injury. In cases of an acute temporary insult, these changes are transient and liver fibrosis may resolve. In chronic liver damage, the injury is sustained, chronic inflammation and accumulation of the extracellular matrix persists, eventually leading to cirrhosis.^{4–7} In NASH, liver fibrosis is closely related to disease progression and mortality.^{6,8–11}

Hepatic stellate cells (HSCs) are liver-specific mesenchymal cells that have a key role in the development of hepatic fibrosis. In response to viral, chemical or immune insults to the liver, the normally quiescent vitamin A storing HSCs undergo a dramatic phenotypic transformation termed “activation” or “trans-differentiation”.^{5,12} When activated this population is responsible for the deposition of the majority of excess

Keywords: C-C motif chemokine ligand 24; CCL24; Antibody; CM-101; Non-alcoholic steatohepatitis; Non-alcoholic fatty liver disease; Fibrosis.

Received 7 March 2019; received in revised form 10 December 2019; accepted 15 December 2019; available online 2 January 2020

* Corresponding author. Address: Kiryat Atidim 7, Tel Aviv, Israel. Tel.: +972773310156, fax: +774448470.

E-mail address: adimor@chemomab.com (A. Mor).



extracellular matrix components that form scar tissue in the fibrotic liver.^{13–15}

The inflammatory response during chronic liver injury is a dynamic process with intrahepatic accumulation of diverse immune cells.¹⁶ Recruitment / infiltration of these cells to the liver and their localization is mainly determined by chemokines and cytokines that are produced by hepatocytes, immune cells, biliary epithelial cells and endothelial cells.¹⁷ Notably, activated HSCs secrete various chemokines, thereby contributing to the ongoing immune response during fibrotic liver diseases.^{15,18} Indeed, the expression of several chemokines and chemokine receptors was shown to be upregulated in the livers of obese patients with severe steatosis and NASH.¹⁹

C-C motif chemokine ligand 24 (CCL24 or eotaxin-2) is a chemokine that promotes cell trafficking and regulates inflammatory and fibrotic activities mainly through the C-C motif chemokine receptor 3 (CCR3) complex. The chemokine is known to be expressed by activated T cells, monocytes, epithelial and endothelial cells as well as by activated fibroblasts.^{20–22} CCL24 induces chemotaxis and activation of CCR3-expressing cells, including immune cells^{23,24} and fibroblasts.²⁵ CCL24 was shown to stimulate human lung fibroblast proliferation and collagen synthesis²⁶ and was found to be associated with the progression of idiopathic pulmonary fibrosis.^{27,28} In *Ccl24* knockout mice, inflammatory cell infiltration into bronchoalveolar lavage fluid was significantly reduced in a model of pulmonary inflammation.²⁹ We recently reported that in the skin and serum of patients with systemic sclerosis both CCL24 and its receptor CCR3 are elevated. Furthermore, we demonstrated that treatment with an anti-CCL24 monoclonal antibody reduced both the inflammatory and fibrotic pathways in pre-clinical models of systemic sclerosis. This anti-inflammatory activity of CCL24 blocking monoclonal antibody was also shown in multiple inflammatory preclinical models, including models of atherosclerosis,³⁰ rheumatoid arthritis³¹ and encephalomyelitis.³²

In the current study, we assessed the potential involvement of the CCL24-CCR3 axis in liver inflammation and fibrosis associated with NAFLD/NASH. We also assessed whether CCL24 blockade could attenuate these processes in the liver.

Materials and methods

Immunohistological evaluation of CCL24 and CCR3 expression in liver biopsies from patients with NASH

Paraffin-embedded liver sections from patients with NASH and healthy controls were obtained from the Royal Free London histopathology archive (REC 07/Q0705) and used for CCL24 detection. The cohort of patients with NASH included 10 biopsies with fibrosis stages of 1 (1 biopsy), 2 (3 biopsies) and 3 (6 biopsies). NAFLD activity scores (NASS) ranged from 4 to 7. The healthy population included livers biopsies from patients that at a clinical review, carried out at the initiation of the study, had no known etiology of liver disease; these biopsies showed normal liver histology. Co-staining of CCL24 with CD68 and of CCR3 with α -SMA [*Acta2*] was carried out using immunofluorescence on commercially available TMA.NASH (Lot #1910017 and #1810052, Sekisui XenoTech) that included both NASH and normal liver biopsies.

Antibodies used for staining included: (i) ChemomAb's proprietary mouse-anti-human CCL24 (CM-101-D8), (ii) CCR3 mAb

(IgG2a mab155 #61828, R&D systems), (iii) α -SMA (Abcam #5694), (iv) CD68 (Abcam #213363).

Measurement of CCL24 levels in serum

Serum CCL24 levels of 20 healthy controls and 51 patients with NAFLD were measured by a commercial ELISA kit for human CCL24 (AB100509, Abcam). Patients with NAFLD were selected from inpatient clinics at the Gastroenterology Department, Kaplan Medical Center, Israel. Patients with NAFLD were identified on the basis of a questionnaire, laboratory investigations, clinical findings and/or ultrasound scan imaging. All regular alcohol consumers were excluded from this study. A complete clinical history, including anthropometric measurements of the participants was obtained. Anthropometric evaluation included measures of body weight, height, and body mass index.

Disorders such as drug-induced liver disease, alcohol-related liver disease, viral hepatitis, Schistosomiasis, autoimmune hepatitis, primary biliary cirrhosis, sclerosing cholangitis, α 1-antitrypsin deficiency, hemochromatosis, Wilson disease and biliary obstruction were excluded. Other exclusion criteria were recent gastrointestinal surgery, pregnancy or suffering from malignancy. Informed consent was obtained from all participants. The group of patients with NAFLD was sub-divided according to the Fibrosis 4 (FIB-4) score, a noninvasive estimate of liver fibrosis with a cut-off of 1.45 ($n = 23$; FIB-4 ≥ 1.45 , $n = 28$; FIB-4 ≤ 1.45).

Individuals who had visited the internal medicine department at Kaplan Medical Center for routine health check-ups without any specific problem and with no abnormality in the clinical and laboratory findings were considered 'normal controls'. Twenty healthy individuals served as controls. None of them had any evidence of fatty liver or previous liver disease.

The ELISA procedure was performed according to manufacturer's instructions. Briefly: serum samples were diluted 1:4 and incubated for 2.5 h at room temperature with gentle shaking. Biotinylated detection antibody was added and incubated for 1 h, then washed. Horseradish peroxidase-streptavidin solution was added for 45 min. ELISA was developed by the addition of 3,3',5,5'-Tetramethylbenzidine substrate for 30 min followed by stop solution. All assays were performed in duplicates and the absorbance was determined using a microplate reader at 450 nm.

The study protocol was approved by National Ethics Committee according to ethics guidelines of the 1975 Declaration of Helsinki, and all patients gave their written informed consent to the study. Helsinki Approval number 0165-15-KMC.

CCR3 expression in peripheral blood mononuclear cells from patients with NAFLD and healthy donors

Peripheral blood mononuclear cells from 35 patients with NAFLD and 22 healthy controls (same cohort used for serum collection, during their annual follow-up visit) were isolated by Ficoll gradient (lymphoprepTM - Axis-Shield # 1114544) and stained for extracellular expression of CCR3 using anti-Human CCR3 PE-conjugated antibody (clone 61828, FAB155P, R&D Systems). CCR3 expression was analyzed using FACS (FACSCalibur BD).

Anti-CCL24 antibody (CM-101)

CM-101 is a proprietary antibody that binds human CCL24 with high affinity. It is a humanized IgG1, kappa light chain monoclonal antibody, manufactured in Chinese hamster ovary cells. The antibody was generated from a parental hybridoma (CM-

101-D8) that contains a murine backbone and cross-reacts with murine CCL24 with high affinity and was used in preclinical models in mice. The humanized CM-101 antibody was used in the rat model.

In vivo animal models

All animal experiments are reported in accordance with the ARRIVE guidance. Studies involving methionine-choline deficient (MCD) diet models were approved by the National Board of Animal Studies in the Ministry of Health by the Kaplan Medical Center. STAM model, study number SLMN081-1704-2 SMC Laboratories, Inc. Japan. The thioacetamide (TAA) model experiments in rats were performed under ethical approval of the "Israel Board for Animal Experiments", approval number IL-17-09-18. Further details regarding the *in vivo* animal models used are provided in the [supplementary information](#).

Ccl24 knockout mice

Ccl24 knockout mice were generated using CRISPR/Cas9-mediated genome engineering by injecting mouse *Ccl24*-gRNA2 (VB150827-10036) targeted to exon 2 of the *Ccl24* gene into fertilized eggs (Cyagen Biosciences Inc). The positive founders (F0) created different chimera mice that were bred to the next generations (with wild-type [WT] C57BL/6) to generate F1 founders. All F1 founder mice were genotyped by PCR and DNA sequencing analysis. Six F1 mice were obtained, 2 with an 8 base pair deletion and 4 with an 11 base pair deletion, both types of deletions creating nonsense mutations in exon 2. F1 mice were then bred to each other to create *Ccl24* knockout mice. Five potential off-target sites have been identified by PCR; DNA sequencing of those PCR amplicons revealed no mutations were found in tested mice.

Analysis of serum biochemistry

For serum biochemistry, blood samples were left at room temperature for 30 min and then centrifuged at 3,500 × g for 10 min at 4°C. The supernatant was collected and stored at -80°C until use. Serum levels of liver enzymes were measured for all animal models using Cobas6000.

Histopathological analyses and immunohistochemistry

Liver tissues were trimmed, fixed in 4% neutral buffered formalin, embedded in paraffin and sectioned at 4 μm thickness. Sections were stained with H&E for histopathological analyses. Steatosis (scale of 0-3), lobular inflammation (scale of 0-3), and ballooning (scale of 0-2); were evaluated for the calculation of NAFLD activity score (NAS) as previously described.³³

Pictures for CCL24 were taken using Zeiss axioskop 40 with attached ICc5 camera (Royal free hospital). TMA slides of CCR3 and α-SMA staining were scanned using Panoramic SCAN (3D Histech). Images were created using CaseViewer software (3D Histech). To assess liver collagen deposition, fixed liver sections were stained using picro-Sirius red solution (Waldeck, Germany). In TAA model, blinded quantification was done for randomly chosen 4 field/section, using Olympus BX-60, DP-73 camera in ×4 magnification (Patho-logica, Israel). Fibrosis area was quantified using digital quantitative morphometry. In STAM model (SMC laboratories Inc., Japan) 5 field/sections were captured around the central vein using a digital camera (DFC295; Leica, Germany) at 200-fold magnification, and the

positive areas in 5 fields/section were measured using ImageJ software (National Institute of Health, USA).

Sircol assessment of liver collagen content

Liver soluble collagen was quantified using the Sircol™ soluble collagen assay (Biocolor, Belfast, UK). The samples were extracted into acid-pepsin solution. The samples were analyzed for collagen content according to the manufacturer's protocol. Briefly, 100 μl of sample was added to 1 ml of the colorimetric reagent (the dye Sirius red in picric acid) and agitated for 30 min followed by centrifugation at 10,000 g for 10 min. The Sirius red dye was released from the pellet with alkali reagent (1 N NaOH) and spectrophotometric readings were taken at 555 nm on a microplate reader. Collagen liver content was calculated as a proportion of total liver weight.

ELISA for CCL24, IL-6 and MMP-9 in liver lysates

Quantification of rat or mouse CCL24, interleukin-6 (IL-6) and matrix metalloproteinase 9 (MMP-9) in liver homogenates was performed using the DuoSet® ELISA kit (DY528, DY406, DY506, and DY8174-05, R&D Systems, Minneapolis, MN). Briefly, liver samples were homogenized using 500 μl extraction buffer for every 0.05 g of liver tissue (extraction buffer -50 mM Tris-HCl 7.6, 150 mM NaCl and protease inhibitor cocktail (Sigma)). Total protein concentration was quantified using the Pierce™ BCA Protein Assay kit (Thermo Scientific) and 300–500 μg total liver protein from each sample was taken to measure CCL24, IL-6 and MMP-9 using ELISA reader (TECAN). Results were analyzed with the Magellan v2.22 software.

Fibrotic gene expression by real-time PCR

Gene expression of *Col1a1*, *Col3a1*, *Acta2*, *Timp1* and *Tgf-β* were tested against GAPDH normalization by Real-time PCR using TaqMan probes (Applied Biosystems #Rn00587558_m1, Rn01775763_g1, Rn01463848_m1, Rn01437681_m1, Rn01759928_g1, Rn00572010_m1). Whole livers were used for RNA isolation (RNeasy® plus Mini kit (Applied Biosystems #74136), 1 μg was taken for cDNA synthesis (Applied Biosystems, high capacity cDNA reverse transcriptase #4368814). cDNA was diluted 1:5 for real-time reaction with the aforementioned probes using QuantStudio™ 1 system for plate reading and QuantStudio™ Design & Analysis software for results analysis.

Assessment of HSC activation

Detection of α-SMA staining and pro-collagen I

LX-2 cells (#SCC064, Millipore) were seeded at a concentration of 1 × 10⁵ cells/ml in growth medium and placed in 6-well plates. Growth medium was replaced by starvation medium (DMEM, 0.5% FCS) after 24 h incubation at 37°C. The following day, CCL24 (100 ng/ml) with or without CM-101 (5, 10 or 15 μg/ml pre-incubated for 1 h) was added to the plates and incubated for an additional 48 h. Cells were harvested and the medium was collected and tested for human pro-collagen I using a commercial ELISA kit (DY6220-05 DuoSet®, R&D systems) according to manufacturer's instructions. Cell pellets were resuspended and α-SMA expression, indicative of cell activation, was assessed in the LX-2 treated cells. Cells were permeabilized and fixed before being stained with anti α-SMA PE-conjugated antibody (IC1420P, R&D systems). Staining was analyzed using FACS (CytoFlex, BECKMAN COULTER).

Scratch motility assay with LX-2

LX-2 cells (10^5 cells/ml) were seeded in a 12-well plate for 24 h followed by change to starvation medium (DMEM+ 0.5% FCS) for an additional 24 h. Next, cells were scratched using a 200 μ l pipette-tip, and changed to treatment medium with CCL24 (25

ng/ml) pre-incubated for 30 min, with or without CM-101 (5 μ g/ml). The scratch was documented at time 0, 24 h and 48 h. The unoccupied area between the 2 scratch edges was assessed and the % of closure was calculated (each treatment was assessed in triplicates).

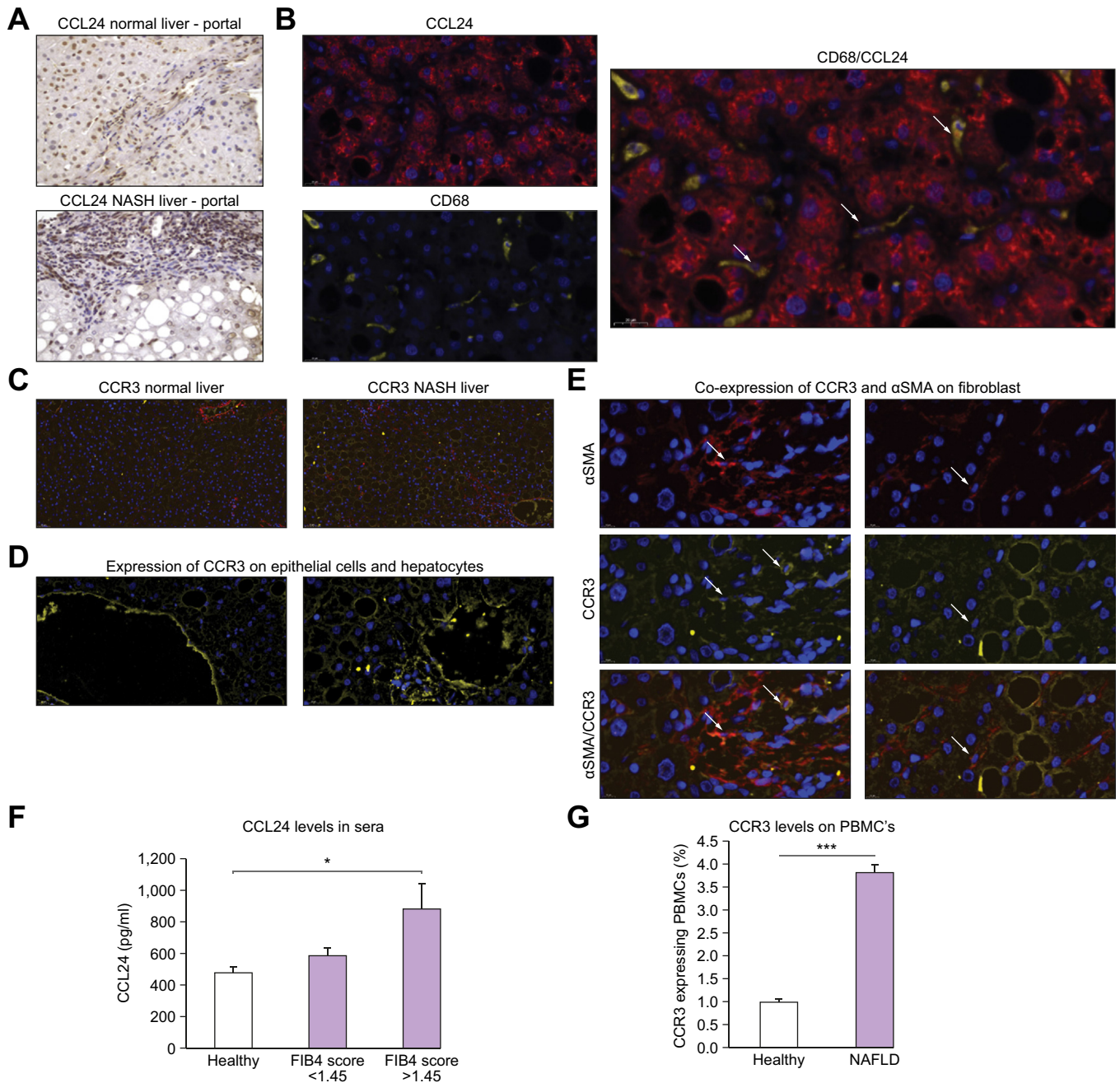


Fig. 1. Significant Expression of CCL24 and its receptor observed in the livers and blood of patients with NAFLD/NASH. (A) Representative pictures of liver histological sections stained for CCL24 (magnification $\times 40$, biopsies were taken from NASH and healthy livers $n = 10$ per group). (B) Representative pictures from double staining of CCL24 and CD68 (macrophage marker) in patients with NASH (magnification $\times 63$, $n = 10$, staining done on TMA). (C) Representative pictures of liver histological samples from TMA stained for CCR3 and α -SMA (total of $n = 7$ samples from NASH, $n = 4$ from healthy livers, magnification $\times 10$). (D) CCR3 expression in epithelial cells and hepatocytes (magnification $\times 40$). (E) Co-staining of CCR3 and α -SMA in patients with NASH, liver biopsies (magnification $\times 100$). (F) Quantitative analysis of CCL24 in sera from healthy donors ($n = 20$) and patients with NAFLD (FIB-4 ≤ 1.45 $n = 27$, FIB-4 ≥ 1.45 $n = 23$). (G) Quantitative analysis of CCR3 in PBMCs from healthy donors ($n = 22$) and patients with NAFLD ($n = 35$); Results are presented as average \pm SE; Student's t test; * $p \leq 0.05$; *** $p \leq 0.001$. FIB-4, Fibrosis-4 score; NAFLD, non-alcoholic fatty liver disease; NASH, non-alcoholic steatohepatitis; PBMCs, peripheral blood mononuclear cells.

Statistical tests

Student's *t* test was used for comparison between 2 groups. *p* <0.05 was considered statistically significant. Results were expressed as mean ± SE.

Results

Expression of CCL24 and its receptor in the liver and serum of patients with NASH/NAFLD

The expression profile and cellular localization of CCL24 in the liver was assessed by immunohistochemistry and immunofluorescent staining on liver biopsies from NASH patients and healthy individuals. Overall, CCL24 positive staining was observed in immune cells, endothelial cells, hepatocytes and cholangiocytes (Fig. 1A). Co-staining of CCL24 together with CD68 demonstrated that CCL24 co-localizes with liver CD68 positive macrophages (Fig. 1B). In accordance with immunohistochemistry, the immunofluorescent staining supported the observation that CCL24 is expressed in hepatocyte nuclei and cytoplasm predominantly in the livers of patients with NASH (Fig. 1B). Moreover, CCL24's receptor, CCR3, was significantly expressed in both lobular and portal areas of the liver, and was specifically seen on endothelial cells, hepatocytes and mesenchymal cells (Fig. 1C and 1D). Importantly, we identified significant co-localization of CCR3 and α-SMA, which further supports the expression of CCR3 on activated fibroblasts (Fig. 1C and 1E) and the relevance of CCR3 to HSC-related activities.

Next, we tested the levels of CCL24 and its receptor in the circulation of patients with NAFLD compared to healthy volunteers. There were significantly higher serum levels of CCL24 in patients with NAFLD compared to healthy volunteers. This elevation was even more pronounced when the NAFLD population was divided to subgroups according to disease

progression (FIB-4 score). CCL24 levels were increased by 2-fold in patients with NAFLD that had FIB-4 scores higher than 1.45, compared to healthy volunteers (Fig. 1F). Similar to the increased CCL24 levels, there was also a 4-fold elevation of CCR3 expression in peripheral blood mononuclear cells isolated from patients with NAFLD compared to healthy volunteers (Fig. 1G).

MCD-diet Induced NASH is attenuated in CCL24 Knockout Mice

To further support the importance of CCL24 in NASH as a single target, we used the experimental MCD-induced steatosis and inflammation model in mice lacking the *Ccl24* gene compared to WT mice. This model is frequently used to study progressive liver pathologies because of its ability to recapitulate steatosis with lobular inflammation and to a lesser extent also fibrosis. Mice lacking the *Ccl24* gene showed an attenuated response to the MCD diet compared to WT mice. Histological assessment revealed significantly lower NAS in *Ccl24* knockout mice than in WT controls. The histological improvement is attributed to reduced scoring in all tested parameters including ballooned hepatocytes, steatosis, and lobular inflammation. Histological assessment in the liver of these mice also revealed significantly reduced fibrosis formation in MCD-fed *Ccl24* knockout mice compared to WT mice (Fig. 2A-C). Serum alanine aminotransferase (ALT) and aspartate aminotransferase (AST), indicative of liver damage, which are elevated in WT mice in response to the MCD diet, were significantly lower in the *Ccl24* knockout animals (Fig. 2 D-F). Another feature seen frequently in MCD diet-fed animals is weight loss. Indeed, both WT and *Ccl24* knockout mice fed with MCD diet exhibited significant weight lost compared to normal chow-fed animals. Nevertheless, *Ccl24* knockout mice demonstrated attenuated weight loss compared to WT mice fed with the MCD diet (Fig. 2G).

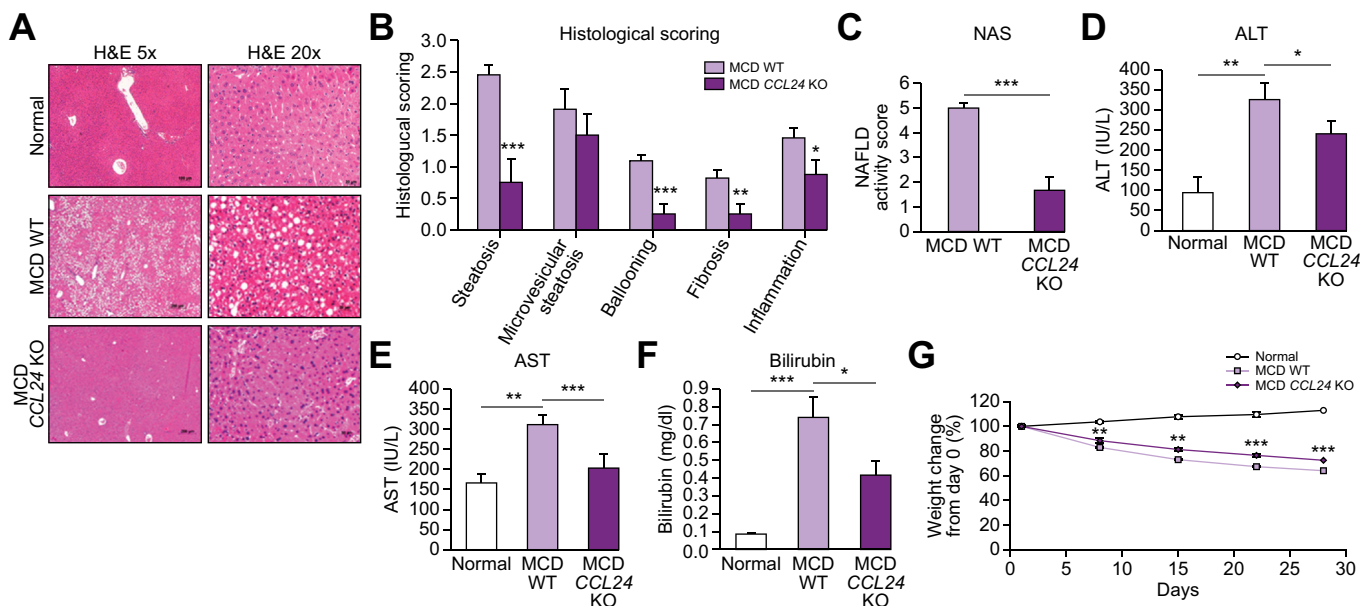


Fig. 2. *Ccl24* knockout mice exhibited an attenuated response to the MCD diet-induced liver damage. (A) Representative H&E stained histological liver samples. Healthy liver from WT control mice (upper panels), MCD-fed WT mice (Middle panels) and MCD-fed *Ccl24* knockout (bottom panels). (B) Histological scoring, comparisons of the 2 MCD-fed groups (WT n = 11 and *Ccl24* knockout n = 8). (C-F) NAS, ALT, AST and bilirubin levels in MCD-induced *Ccl24* knockout mice compared to WT mice. (G) Average percentage weight change in normal, MCD diet-fed WT and *Ccl24* knockout mice. Results are presented as average ± SE; Student's *t* test; **p* <0.05, ***p* <0.01, ****p* <0.001. ALT, alanine aminotransferase; AST, aspartate aminotransferase; MCD, methionine–choline deficient; NAS, non-alcoholic fatty liver disease activity score; WT, wild-type.

Blockade of CCL24 using monoclonal antibody inhibits NASH-related pathologies in the MCD-diet mice model

To further elucidate the involvement of CCL24 in the MCD model, we employed this model on WT mice treated with a monoclonal antibody that blocks CCL24 activity. We compared WT mice fed with normal chow diet or MCD diet and either treated with 5 mg/kg CM-101 (D8) or vehicle control (Fig. 3). While the MCD diet induced NASH-related histological features (steatosis, inflammation and hepatocyte ballooning) in untreated mice, treatment of MCD-fed mice with 5 mg/kg CM-101 (D8) from day 10 significantly improved the histological scoring by 34% (Fig. 3A-B). Furthermore, elevated levels of AST, ALT and bilirubin observed in the MCD-diet fed group were significantly reduced in MCD mice treated with CM-101 (D8) (Fig. 3C-E). Moreover, MCD-fed mice had significantly higher CCL24 levels in the liver with a 40% elevation compared to mice fed with normal chow diet (3.87 ± 0.17 compared to 2.74 ± 0.13 ng/mg total protein). CCL24 level was normalized following CM-101 (D8) treatment (2.73 ± 0.13 ng/mg total protein). These results

provide further evidence of the connection between liver pathology and CCL24 expression/regulation.

CM-101 (D8) improves parameters of liver damage in experimental murine STAM model

To substantiate the role of CCL24 in NASH pathogenesis and the ability of CM-101 to interfere with induced liver damage, we utilized the well-established commercial murine STAM model (Fig. 4).³⁴ As previously reported, STAM mice exhibited many NASH-related features including: micro- and macrovesicular fat deposition, hepatocellular ballooning and inflammatory cell infiltration.³⁵ STAM mice treated with 5 mg/kg CM-101 (D8), exhibited a significant 30% decrease in NAS, mostly attributed to reduced inflammation and steatosis ($p < 0.05$ vs. controls, Fig. 4A-4D). Moreover, in accordance with reduced fibrosis in MCD mice, CM-101 (D8) significantly reduced pericentral collagen deposition and fibrosis in STAM mice, indicated by a 50% decrease in Sirius red staining compared to control mice (Fig. 4E and 4F).

To explore the reduced inflammatory-fibrotic phenotype seen in CM-101 (D8)-treated STAM mice, we evaluated IL-6 levels in the liver of both control and CM-101 (D8) treated animals. Along with reduced inflammation and fibrosis, a significant (62%) reduction of liver IL-6 levels was observed in CM-101 (D8)-treated animals compared to controls (Fig. 4G).

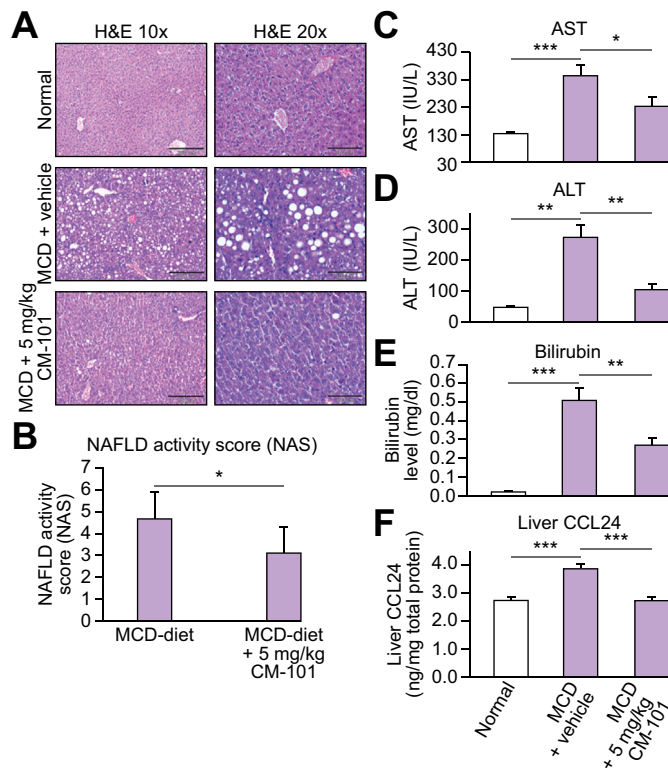


Fig. 3. Anti-CCL24 antibody (CM-101 (D8)) reduced NASH-related pathologies in the MCD-diet mouse model (treatment mode). (A) Representative H&E stained histological liver samples. Healthy liver from chow diet-fed mice (upper panels), MCD-fed WT mice (middle panels) and MCD + 5 mg/kg CM-101 (D8) treated group (bottom panels). (B) Histological scoring, comparisons of the 2 groups fed with the MCD diet (MCD diet and MCD diet + 5 mg/kg CM-101 (D8), $n = 8$). (C-E) AST, ALT and bilirubin levels in the MCD-induced NASH model compared to MCD + 5 mg/kg CM-101 (D8) treated group. (F) CCL24 levels in the liver measured by ELISA using total protein liver lysates from chow diet-fed mice, MCD-fed WT mice and MCD + 5 mg/kg CM-101 (D8) treated mice. Results are presented as average \pm SE; Student's t test; * $p \leq 0.05$, ** $p \leq 0.01$, *** $p \leq 0.001$. ALT, alanine aminotransferase; AST, aspartate aminotransferase; MCD, methionine-choline deficient; NAS, non-alcoholic fatty liver disease activity score; WT, wild-type.

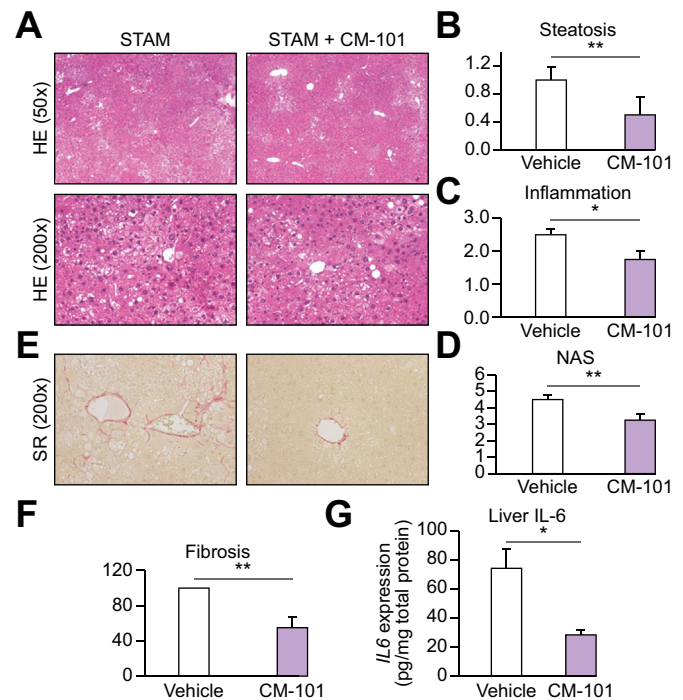


Fig. 4. CM-101 (D8) improved key parameters of liver damage in experimental NASH in STAM model in mice (treatment mode). (A) Representative images of H&E stained liver sections from STAM and STAM + CM-101 (D8) treated groups. (B-D) Quantification of steatosis, inflammation and NAS in the STAM and STAM + CM-101(D8) treated groups, ($n = 8$). (E) Representative Sirius red stained liver sections. (F) Sirius red quantification in the CM-101 (D8) treated animal compared to vehicle, ($n = 8$). (G) Quantification of IL-6 expression in the liver following CM-101 (D8) treatment compared to vehicle. Student's t test; * $p \leq 0.05$, ** $p \leq 0.01$. NAS, non-alcoholic fatty liver disease activity score; NASH, non-alcoholic steatohepatitis; SR, Sirius red.

CCL24 blockade robustly attenuates liver fibrosis in the TAA rat model

Both MCD and STAM models represent mainly the steatosis-inflammatory arms of NASH pathology and induced only limited fibrotic scarring. To further elucidate the role of CCL24 in the establishment of fibrosis and assess the ability of CM-101 to interfere with liver fibrosis by blocking CCL24, we employed the widely used TAA model of fibrosis in rats. Similar to previous publications, we found that livers from rats treated with TAA for 8 weeks exhibit extensive fibrosis visible upon gross examination, marked elevations of liver enzymes and elevated collagen content.³⁵ The CM-101-treated group exhibited a dramatic decrease in liver fibrosis compared to the vehicle-treated group (Fig. 5). CM-101-treated rats demonstrated almost no visible features of fibrosis macroscopically (Fig. 5A) and exhibited significantly lower liver enzyme levels (Fig. 5B). Histological evaluation

showed significantly reduced fibrosis in the livers of rats treated with CM-101 (Fig. 5C), indicated by an 80% reduction in Sirius red collagen staining compared to the vehicle-treated group, as well as a reduction of liver collagen measured by sircol (Fig. 5D and 5E).

In addition, we measured the effect of CM-101 on 2 factors involved in liver fibrosis, MMP-9 and IL-6. MMP-9 is known to activate HSCs and induce their trans-differentiation by activating TGF- β ,^{36,37} while IL-6 is a central inflammatory cytokine in the liver that can also activate HSCs and was found to correlate with increased fibrosis.³⁸ TAA induced a significant upregulation of both MMP-9 and IL-6 in the livers of treated rats compared to untreated controls. Treatment with CM-101 normalized protein levels of MMP-9 and IL-6 to the levels seen in healthy rats (Fig. 5F and 5G).

To support the histological evidence of fibrosis, mRNA levels of profibrotic genes were measured in the liver of treated and

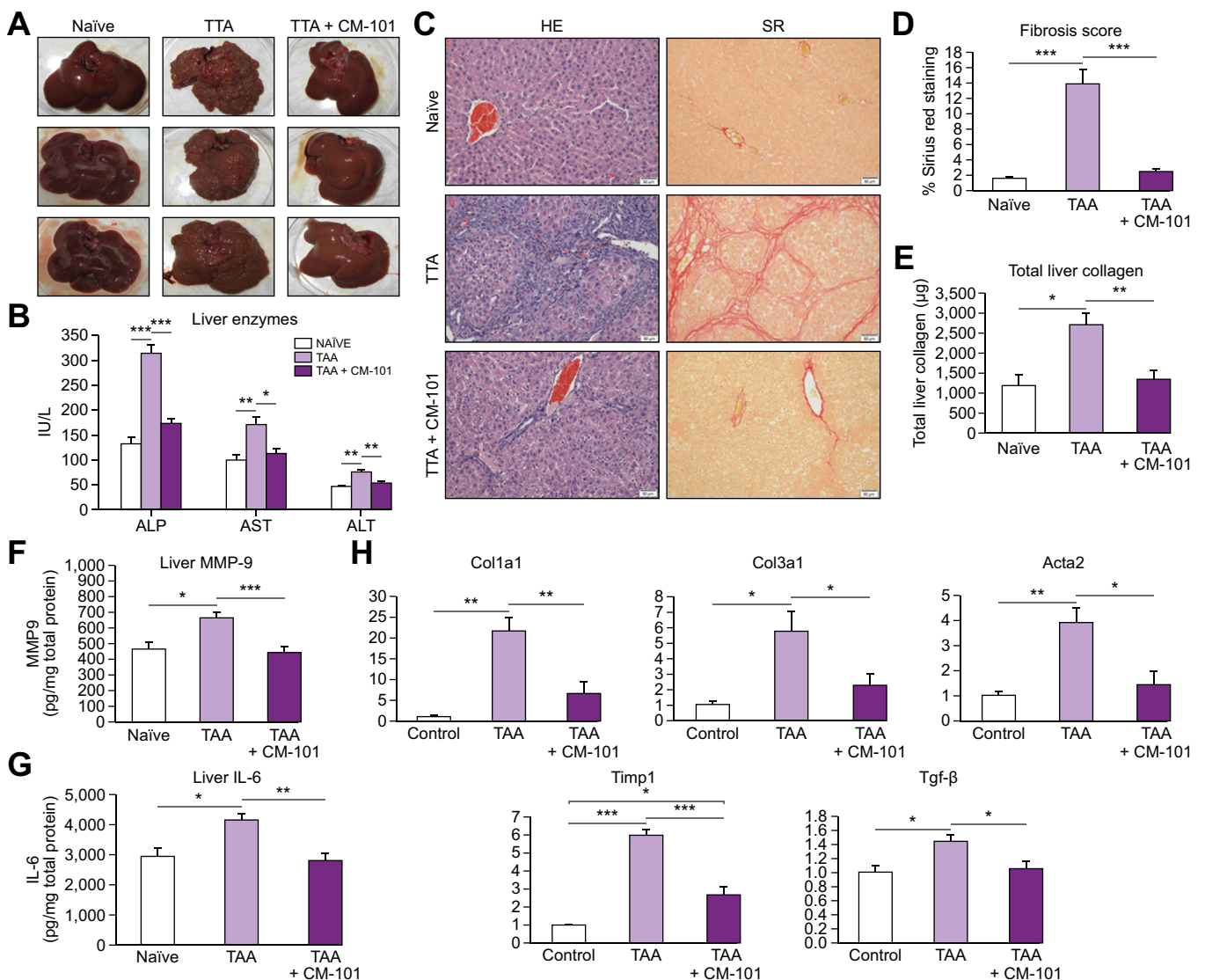


Fig. 5. Anti-CCL24 monoclonal antibody attenuated liver fibrosis in the TAA rat treatment model (treatment mode). (A) Macroscopic examination of naive (n = 5), TAA-treated animals for 8 weeks without or with 2.5 mg/kg CM-101 from week 4-8 (n = 10). (B) Serum liver enzymes levels in the different groups (C) Representative photographs of H&E and Sirius red-stained liver sections in the different groups (D-E) Sirius red quantification (fibrosis score) and collagen measured by sircol exemplified in the different groups. (F-G) Protein levels of IL-6 and MMP-9 quantified in the liver from different groups. (H) Expression of fibrotic genes in livers by real-time PCR. Student's *t* test; **p* ≤ 0.05; ***p* ≤ 0.01; ****p* ≤ 0.001; SR, Sirius red; TAA, thioacetamide.

control animals. *Col1a1*, *Col3a1*, *Acta2*, *Timp1* and *Tgf- β* genes that represent the severe fibrotic damage seen in this model, were all markedly increased in TAA-treated animals. In CM-101-treated rats all 5 fibrotic genes, in accordance with histological assessment, were either significantly reduced or completely normalized to basal levels quantified in the healthy animals. *Col1a1* increased most robustly by 21.7 ± 3.13 after TAA treatment. CM-101 reduced this elevation by 70% to 6.6 ± 2.78 . *Col3a1* was increased by 5.8 ± 1.29 and reduced following CM-101 treatment by 60% to 2.3 ± 0.76 . *Acta2*, a well-known marker of fibroblast activation, was increased by 3.9 ± 0.58 -fold, while CM-101 reduced its levels by 65% to 1.4 ± 0.55 . *Timp1* was increased by 6 ± 0.34 -fold after TAA and reduced to 2.7 ± 0.47 following CM-101 treatment. Finally, *Tgf- β* was also increased by 1.4 ± 0.1 following TAA and normalized back to 1.1 ± 0.11 in the TAA CM-101 treated animals (Fig. 5H).

Profibrogenic effects of human HSCs induced by CCL24 are attenuated by CM-101 *in vitro*

HSCs are the main contributors to liver fibrosis producing most of the extracellular matrix deposition which forms the fibrotic scar. To evaluate whether the CM-101-mediated antifibrotic effect observed in the animal models was the result of a direct effect on HSCs, we used the human HSC cell line, LX-2.³⁹ HSC motility is a well-known indicator of activation⁴⁰ and therefore we tested the ability of CCL24 to induce HSC motility using a scratch assay. LX-2 cell motility was induced following treatment with CCL24 (25 ng/ml) at both 24 h and 48 h after scratch. This enhancement in motility was completely reversed by pre-incubation of CCL24 with 5 μ g/ml CM-101 (Fig. 6A).

In addition, treating LX-2 cells with CCL24 robustly and significantly increased α -SMA expression as well as pro-collagen I secretion compared to untreated cells. Pre-incubation of CCL24 (100 ng/ml) with 5-15 μ g/ml CM-101 robustly attenuated HSC activation, as indicated by normalization of α -SMA to levels seen in cells not treated with CCL24, and reduced pro-collagen I secretion (Fig. 6B and 6C).

Discussion

Chemokines are traditionally described as proinflammatory regulators due to their ability to induce chemotaxis of immune cells into diseased organs. Over the past decade, the role of chemokines in different cellular pathologies was further elucidated, demonstrating that chemokines play an important role in additional cellular processes including fibrosis.^{14,17}

Chemokines were found to correlate with disease pathology in several systems and their association with the severity of disease made them desirable drug targets and possible biomarkers.

CCL24 is a chemokine that was mainly investigated in the past for its ability to promote allergic responses, due to the prominent expression of its receptor CCR3 on eosinophils.^{23,29} Interestingly, it was also found that CCL24 plays a significant role in promoting skin and lung fibrotic processes by directly effecting fibroblast activation and being involved in an inflammatory response that supports fibrosis.^{25,26,41,42}

In the present study we show for the first time that CCL24 plays a central role in the development of intrahepatic fibrosis and liver damage. CCL24, as well as its receptor CCR3, were found to be significantly expressed in the liver and peripheral blood cells of patients with NAFLD and NASH. Both CCL24 and

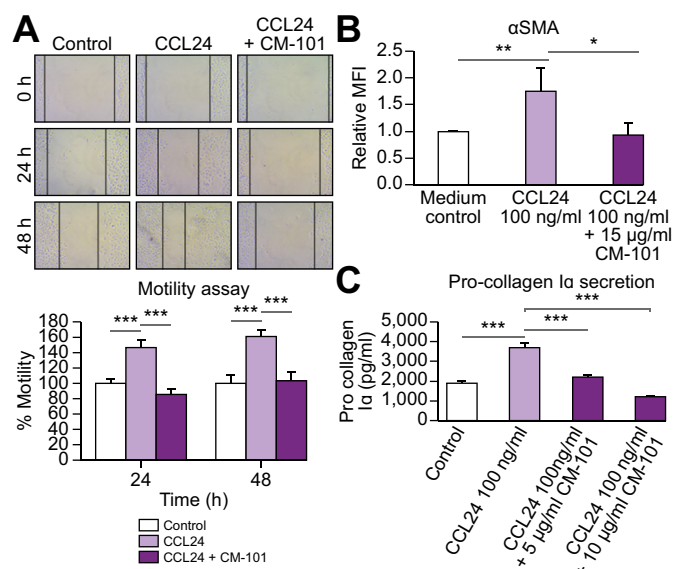


Fig. 6. CM-101 suppressed CCL24-induced activation of HSCs *in vitro*. (A) Representative images and quantification of HSC (LX-2 cell line) scratch assay. Images of scratched wells were taken at time 0 h, 24 h and 48 h. Percentage closure of scratched area was evaluated for control group or cells treated with CCL24 (25 ng/ml) with or without CM-101 (5 μ g/ml). (B) α -SMA expression measured by FACS following treatment with CCL24, with or without CM-101 (C) Pro-collagen I alpha secretion was quantified with a commercial ELISA kit, following activation of HSCs with CCL24 (100 ng/ml, 48 h incubation) with or without CM-101. Student's *t* test; **p* \leq 0.01, ***p* \leq 0.005, ****p* \leq 0.001, each graph represents an average of 3 different experiments. HSCs, hepatic stellate cells; MFI, median fluorescence intensity.

CCR3 are broadly expressed in both parenchymal and non-parenchymal cells in the livers of patients with NASH and are not exclusively expressed by immune cells.

Using the experimental MCD-induced NASH model in *Ccl24* knockout mice, we further validated the role of CCL24 as a single target in NASH development. The robust attenuation of disease parameters in the absence of CCL24 compared with WT controls suggests that the CCL24-CCR3 axis might have an important role in regulating the inflammatory fibrotic axis involved in liver damage.

In accordance with the co-localization of CCR3 and α -SMA on hepatic fibroblast, the human LX2 cells express CCR3, thus enabling these cells to sense and respond to CCL24. Indeed, we found that CCL24 induces activation of these cells and that the CCL24 blocking antibody CM-101 blocked CCL24-induced activation by reducing motility, α -SMA expression and pro-collagen I secretion. These results suggest that CM-101 treatment can mitigate HSC activation, thereby potentially alleviating the fibrotic injury seen in experimental models and ultimately in patients.

The anti-inflammatory and antifibrotic properties of blocking CCL24 in models of atherosclerosis, systemic sclerosis and idiopathic pulmonary fibrosis were previously shown.^{30-32,42} In this publication we demonstrate that CCL24 also plays a significant role in liver fibrosis primarily by influencing fibroblasts. These results imply that CCL24 influences fibroblast activation in a dual pathway, primarily by acting directly on fibroblast activation through the CCR3 receptor, but also via an augmented inflammatory response. Moreover, it is well known that activated HSCs can also secrete inflammatory mediators that

enhance tissue damage resulting in sustained and chronic inflammatory fibrotic injury.^{12,13,40} Targeting CCL24 in chronic uncontrolled fibrotic processes can therefore be highly effective by influencing several cell compartments. In this study, we show that even under severe fibrotic insult in the TAA rat model, treatment with CM-101 led to robust reduction in liver injury and fibrosis. Interestingly, and consistent with the putative mechanism of action of CM-101, hepatic levels of MMP-9 and IL-6, that are known to be upregulated in this model, involved in both the inflammatory and fibrotic processes, were significantly attenuated following treatment with CM-101. It is conceivable that a positive feedback loop consisting of proinflammatory and profibrotic cytokine/chemokine bursts occurs locally in NASH livers, perpetuating HSC activation and driving fibrosis. CM-101 appears to interfere significantly with this 'vicious' cycle by attenuating both the proinflammatory and profibrotic signals.

Additionally, CCL24 staining in human liver biopsies revealed a novel finding, showing its expression in human hepatocytes. This is supported by real-time PCR data from human hepatocytes (ChemomAb, unpublished data).

Furthermore, using both MCD and STAM experimental NASH models we showed that inhibition of CCL24 by CM-101 (D8) profoundly attenuated hepatocyte damage. Treatment with CM-101 (D8) decreased steatosis, microvesicular steatosis and hepatocyte ballooning, leading to a vast improvement in liver injury parameters. This hepatocyte-related effect was shown to be relevant for other chemokines and chemokine receptors. For example, Kim *et al.* recently reported that CCR5 is expressed on hepatocytes and is involved in their ability to accumulate fat and promote steatosis and that CCL5 is secreted by hepatocytes during steatosis.^{43–45} Our data suggest that there might be a direct effect of CCL24 on hepatocytes, although an indirect effect could not be completely ruled out. This effect, either direct or indirect, is novel and highly interesting and needs to be further elucidated in upcoming research on CCL24.

Taken together, the preclinical data presented in this publication suggest that while CCL24 is significantly involved in promoting processes that induce liver fibrosis and inflammation, its blockade using a monoclonal antibody can potentially be utilized as an antifibrotic agent in liver diseases.

Abbreviations

α -SMA, α -smooth muscle actin; ALT, alanine aminotransferase; AST, aspartate aminotransferase; CCL24, C-C motif chemokine ligand 24; CCR3, C-C motif chemokine receptor 3; HSCs, hepatic stellate cells; IL-6, interleukin-6; MCD, methionine-choline deficient; MFI, median fluorescence intensity; MMP, matrix metalloproteinase; NAFLD, non-alcoholic fatty liver disease; NAS, NAFLD activity score; NASH, non-alcoholic steatohepatitis; PBMC, peripheral blood mononuclear cells; TAA, thioacetamide; WT, wild-type.

Financial support

The work described in this paper was funded by ChemomAb Ltd.

Conflict of interest

Please refer to the accompanying ICMJE disclosure forms for further details.

Authors' contributions

M.S.-S, N.B and A.M designed the experiments. M.S.-S, N.B, A.K and V.E performed the experiments. D.H and Y.M provided human serum samples and clinical data, A.H performed the immune-histological work in human tissues. A.A and S.H reviewed the manuscript and analyzed the data, M.P, J.G and S.F critically reviewed the manuscript and consulted on studies design. A.M wrote the manuscript.

Supplementary data

Supplementary data to this article can be found online at <https://doi.org/10.1016/j.jhepr.2019.100064>.

References

Author names in bold designate shared co-first authorship

- [1] Chalasani N, Younossi Z, Lavine JE, Charlton M, Cusi K, Rinella M, et al. The diagnosis and management of nonalcoholic fatty liver disease: practice guidance from the American Association for the Study of Liver Diseases. *Hepatology* 2018;67:328–357.
- [2] Konerman MA, Jones JC, Harrison SA. Pharmacotherapy for NASH: current and emerging. *J Hepatol* 2018;68:362–375.
- [3] Friedman SL, Neuschwander-Tetri BA, Rinella M, Sanyal AJ. Mechanisms of NAFLD development and therapeutic strategies. *Nat Med* 2018;24:908–922.
- [4] Friedman SL. Mechanisms of hepatic fibrogenesis. *Gastroenterology* 2008;134:1655–1669.

- [5] Friedman SL. Hepatic fibrosis: emerging therapies. *Dig Dis* 2015;33:504–507.
- [6] Popov Y, Schuppan D. Targeting liver fibrosis: strategies for development and validation of antifibrotic therapies. *Hepatology* 2009;50:1294–1306.
- [7] Younossi ZM, Loomba R, Anstee QM, Rinella ME, Bugianesi E, Marchesini G, et al. Diagnostic modalities for nonalcoholic fatty liver disease, nonalcoholic steatohepatitis, and associated fibrosis. *Hepatology* 2018;68:349–360.
- [8] Angulo P, Kleiner DE, Dam-Larsen S, Adams LA, Bjornsson ES, Charatcharoenwithaya P, et al. Liver fibrosis, but no other histologic features, is associated with long-term outcomes of patients with nonalcoholic fatty liver disease. *Gastroenterology* 2015;149:389–397.e10.
- [9] Dulai PS, Singh S, Patel J, Soni M, Prokop LJ, Younossi Z, et al. Increased risk of mortality by fibrosis stage in nonalcoholic fatty liver disease: systematic review and meta-analysis. *Hepatology* 2017;65:1557–1565.
- [10] Ekstedt M, Hagstrom H, Nasr P, Fredrikson M, Stal P, Kechagias S, et al. Fibrosis stage is the strongest predictor for disease-specific mortality in NAFLD after up to 33 years of follow-up. *Hepatology* 2015;61:1547–1554.
- [11] LaBrecque DR, Abbas Z, Anania F, Ferenci P, Khan AG, Goh KL, et al. World Gastroenterology Organisation global guidelines: nonalcoholic fatty liver disease and nonalcoholic steatohepatitis. *J Clin Gastroenterol* 2014;48:467–473.
- [12] Higashi T, Friedman SL, Hoshida Y. Hepatic stellate cells as key target in liver fibrosis. *Adv Drug Deliv Rev* 2017;121:27–42.
- [13] Puche JE, Saiman Y, Friedman SL. Hepatic stellate cells and liver fibrosis. *Compr Physiol* 2013;3:1473–1492.
- [14] Wick G, Grundtman C, Mayerl C, Wimpfing TF, Feichtinger J, Zelger B, et al. The immunology of fibrosis. *Annu Rev Immunol* 2013;31:107–135.
- [15] Parola M, Pinzani M. Liver fibrosis: pathophysiology, pathogenetic targets and clinical issues. *Mol Aspects Med* 2019;65:37–55.
- [16] Ju C, Tacke F. Hepatic macrophages in homeostasis and liver diseases: from pathogenesis to novel therapeutic strategies. *Cell Mol Immunol* 2016;13:316–327.
- [17] Marra F, Tacke F. Roles for chemokines in liver disease. *Gastroenterology* 2014;147:577–594 e571.
- [18] Friedman SL. Hepatic stellate cells: protean, multifunctional, and enigmatic cells of the liver. *Physiol Rev* 2008;88:125–172.
- [19] Bertola A, Bonnafant S, Anty R, Patoureaux S, Saint-Paul MC, Iannelli A, et al. Hepatic expression patterns of inflammatory and immune response genes associated with obesity and NASH in morbidly obese patients. *PLoS One* 2010;5:e13577.
- [20] Ancuta P, Autissier P, Wurcel A, Zaman T, Stone D, Gabuzda D. CD16+ monocyte-derived macrophages activate resting T cells for HIV infection by producing CCR3 and CCR4 ligands. *J Immunol* 2006;176:5760–5771.
- [21] Diny NL, Hou X, Barin JG, Chen G, Talor MV, Schaub J, et al. Macrophages and cardiac fibroblasts are the main producers of eotaxins and regulate eosinophil trafficking to the heart. *Eur J Immunol* 2016;46:2749–2760.

- [22] Heiman AS, Abonyo BO, Darling-Reed SF, Alexander MS. Cytokine-stimulated human lung alveolar epithelial cells release eotaxin-2 (CCL24) and eotaxin-3 (CCL26). *J Interferon Cytokine Res* 2005;25:82–91.
- [23] Forssmann U, Ugucioni M, Loetscher P, Dahinden CA, Langen H, Thelen M, et al. Eotaxin-2, a novel CC chemokine that is selective for the chemokine receptor CCR3, and acts like eotaxin on human eosinophil and basophil leukocytes. *J Exp Med* 1997;185:2171–2176.
- [24] Manousou P, Kolios G, Valatas V, Drygiannakis I, Bourikas L, Pyrovolaki K, et al. Increased expression of chemokine receptor CCR3 and its ligands in ulcerative colitis: the role of colonic epithelial cells in in vitro studies. *Clin Exp Immunol* 2010;162:337–347.
- [25] Buskermolen JK, Roffel S, Gibbs S. Stimulation of oral fibroblast chemokine receptors identifies CCR3 and CCR4 as potential wound healing targets. *J Cell Physiol* 2017;232:2996–3005.
- [26] Kohan M, Puxeddu I, Reich R, Levi-Schaffer F, Berkman N. Eotaxin-2/CCL24 and eotaxin-3/CCL26 exert differential profibrogenic effects on human lung fibroblasts. *Ann Allergy Asthma Immunol* 2010;104:66–72.
- [27] Amubieya OO, Kim GHJ, Huynh R, Shino M, DerHovanessian A, Sayah D, et al. Eotaxin-2 in lung tissue is associated with disease severity and progression of IPF. In C37. *Pulmonary Fibrosis Am Thorac Soc* 2016;1–307:A4950.
- [28] Foster MW, Morrison LD, Todd JL, Snyder LD, Thompson JW, Soderblom EJ, et al. Quantitative proteomics of bronchoalveolar lavage fluid in idiopathic pulmonary fibrosis. *J Proteome Res* 2015;14:1238–1249.
- [29] Pope SM, Zimmermann N, Stringer KF, Karow ML, Rothenberg ME. The eotaxin chemokines and CCR3 are fundamental regulators of allergen-induced pulmonary eosinophilia. *J Immunol* 2005;175:5341–5350.
- [30] Mor A, Afek A, Entin-Meer M, Keren G, George J. Anti eotaxin-2 antibodies attenuate the initiation and progression of experimental atherosclerosis. *World J Cardiovasc Dis* 2013;3:339–346.
- [31] Ablin JN, Entin-Meer M, Aloush V, Oren S, Elkayam O, George J, et al. Protective effect of eotaxin-2 inhibition in adjuvant-induced arthritis. *Clin Exp Immunol* 2010;161:276–283.
- [32] **Mausner-Fainberg K, Karni A, George J, Entin-Meer M, Afek A.** Eotaxin-2 blockade ameliorates experimental autoimmune encephalomyelitis. *World J Immunol* 2013;3(1):7–14.
- [33] Kleiner DE, Brunt EM, Van Natta M, Behling C, Contos MJ, Cummings OW, et al. Design and validation of a histological scoring system for nonalcoholic fatty liver disease. *Hepatology* 2005;41:1313–1321.
- [34] Fujii M, Shibasaki Y, Wakamatsu K, Honda Y, Kawauchi Y, Suzuki K, et al. A murine model for non-alcoholic steatohepatitis showing evidence of association between diabetes and hepatocellular carcinoma. *Med Mol Morphol* 2013;46:141–152.
- [35] Lefebvre E, Moyle G, Reshef R, Richman LP, Thompson M, Hong F, et al. Antifibrotic effects of the dual CCR2/CCR5 antagonist cenicriviroc in animal models of liver and kidney fibrosis. *PLoS One* 2016;11:e0158156.
- [36] Feng M, Ding J, Wang M, Zhang J, Zhu XH, Guan WX. Kupffer-derived matrix metalloproteinase-9 contributes to liver fibrosis resolution. *Int J Biol Sci* 2018;14:1033–1040.
- [37] Kobayashi T, Kim H, Liu X, Sugiura H, Kohyama T, Fang Q, et al. Matrix metalloproteinase-9 activates TGF-beta and stimulates fibroblast contraction of collagen gels. *Am J Physiol Lung Cell Mol Physiol* 2014;306:L1006–1015.
- [38] Kagan P, Sultan M, Tachlytski I, Safran M, Ben-Ari Z. Both MAPK and STAT3 signal transduction pathways are necessary for IL-6-dependent hepatic stellate cells activation. *PLoS One* 2017;12:e0176173.
- [39] Xu L, Hui AY, Albanis E, Arthur MJ, O'Byrne SM, Blaner WS, et al. Human hepatic stellate cell lines, LX-1 and LX-2: new tools for analysis of hepatic fibrosis. *Gut* 2005;54:142–151.
- [40] **Schwabe RF, Batailler R, Brenner DA.** Human hepatic stellate cells express CCR5 and RANTES to induce proliferation and migration. *Am J Physiol Gastrointest Liver Physiol* 2003;285:G949–958.
- [41] Matucci-Cerinic M, Katav, A., Segal-Salto, A., Levy, Y., & Mor, A. A novel antibody blocking CCL24/CCR3 reduces chemokines of immune cells and the transition of fibroblasts to myofibroblasts in systemic sclerosis "SSc. In 4th Systemic Sclerosis World Congress 2016.
- [42] Mor A, Segal Salto M, Katav A, Barashi N, Edelshtein V, Manetti M, et al. Blockade of CCL24 with a monoclonal antibody ameliorates experimental dermal and pulmonary fibrosis. *Ann Rheum Dis* 2019;78:1260–1268.
- [43] Kim BM, Abdelfattah AM, Vasan R, Fuchs BC, Choi MY. Hepatic stellate cells secrete Ccl5 to induce hepatocyte steatosis. *Sci Rep* 2018;8:7499.
- [44] **Li BH, He FP,** Yang X, Chen YW, Fan JG. Steatosis induced CCL5 contributes to early-stage liver fibrosis in nonalcoholic fatty liver disease progress. *Transl Res* 2017;180:103–117.e4.
- [45] **Kirovski G, Gabele E,** Dorn C, Moleda L, Niessen C, Weiss TS, et al. Hepatic steatosis causes induction of the chemokine RANTES in the absence of significant hepatic inflammation. *Int J Clin Exp Pathol* 2010;3:675–680.